



# Characteristics and Manufacturability of Duplex Stainless Steel: A Review

S. Patra<sup>1</sup> · A. Agrawal<sup>2</sup> · A. Mandal<sup>3</sup> · A. S. Podder<sup>2</sup>

Received: 2 April 2021 / Accepted: 25 April 2021 / Published online: 13 May 2021  
© The Indian Institute of Metals - IIM 2021

**Abstract** Duplex stainless steels (DSS) have been growing continuously as they are cost effective alternative to austenitic stainless steel with better mechanical and corrosion resistance. Duplex stainless steel compositions are expanding in both directions towards leaner and richer chemistry for popular as well as very critical applications. The strength of DSS is its high yield strength compared to popular austenitic series and corrosion resistance particularly pitting and chloride stress corrosion cracking. Challenges of DSS remain in the embrittlement phase formation during the manufacturing of highly alloyed DSS, hot cracking and formability of the steel. Super duplex and hyper duplex steels are finding extremely critical application due to their good mechanical properties and corrosion resistance even replacing Nickel based alloys and Ti alloys in few applications. The paper reviews the characteristics and manufacturability of duplex stainless steel including recent developments.

**Keywords** Duplex stainless steel · Manufacturing · Application · Corrosion

## 1 Introduction

Duplex stainless steel (DSS), the newest member of the stainless steel family, is being commercially produced for more than 50 years [1, 2]. The steel has grown at a rate of about 4.7% in between 2016 and 2021 [3]. It is primarily used in oil & gas, chemical process industry, pulp & paper, mining, nuclear, and many other industries [1, 4, 5]. Duplex stainless steel consists of about an equal percentage of ferrite and austenite in the microstructure. At first, 2205 DSS (22Cr-5Ni-3Mo) has been developed and it is the most popular of all duplex stainless steel till now consisting of about 50% of duplex production. Then leaner as well as a richer variant of DSS was developed based on the requirement of corrosion resistance and cost-effectiveness [1, 2]. Austenitic stainless steel especially popular 304 and 316 grade can be replaced by leaner and popular duplex stainless steel as similar corrosion resistance and higher mechanical properties can be achieved with those alloys along with cheaper raw material costing coming from Ni saving. Table 1 shows the different duplex stainless steel and their chemical composition and typical mechanical properties. Like the leaner version, super duplex stainless steel (SDSS) can be used in a highly corrosive medium and can replace highly alloyed super austenitic stainless steel [6]. Recently developed hyper duplex stainless steels possess the highest corrosion resistance among all the stainless steel and alloy steels and can even replace Ni-based alloys in terms of cost-effective corrosion protection application [7]. Due to high resistance to stress corrosion cracking, duplex stainless steel replaces many 300 series alloys in applications like Hydrocarbon condensate heat exchanger, Maleic anhydride heat exchanger, Margarine plant, Copper electrolyte, Ammonia chloride, a Methanol plant, Fatty acids and Polyethylene plant, etc. [8].

✉ S. Patra  
psudiptapatra@gmail.com

<sup>1</sup> Indian Institute of Technology (BHU), Varanasi 221005, India

<sup>2</sup> Jindal Stainless Limited, Hisar, Haryana 125005, India

<sup>3</sup> Indian Institute of Technology, Kharagpur, West Bengal, India

**Table 1** Chemical composition of popular duplex stainless steels

Grade	Cr	Mn	Ni	C	N	Si	Cu	Mo	W	Creq	Nieq	Creq/Nieq	PREN	YS (Mpa)	UTS (Mpa)	%El
2101	21	5	1.5	0.02	0.23	0.4	0.3	0.2		21.2	9.075	2.34	25.34	600	700	30
2304	23	1.5	4	0.02	0.13	0.4	0.3	0.3		23.3	8.575	2.72	26.07	450	650	35
2205	22	1	5	0.02	0.15	0.4	0.3	3		25	10.18	2.46	34.3	480	680	35
2507	25	1	7	0.02	0.25	0.4	0.2	3.5		28.5	15.15	1.88	40.55	620	800	30
32,760	25	0.6	7	0.02	0.25	0.4	0.6	3.5	0.6	28.5	15.25	1.87	40.55	620	800	30
2707	27	0.8	7	0.02	0.4	0.4	0.4	5		32	19.7	1.62	49.9	700	850	30

But the challenges of duplex stainless steels are mainly its processing, especially hot ductility of the DSS is poor [9–12]. As the hot ductility is very poor, hot rolling to thinner section is difficult, and thus to get cold rolled annealed pickled product of thinner gauge requires multiple steps of cold rolling and annealing. Also, embrittlement phase formation during hot processing is a problem in DSS. As the Cr and Mo increase, the formation of sigma, chi, and other phase formation is also increased. Welding of DSS was a long back problem, but with the addition of nitrogen, the phase fraction in DSS can be achieved in the desired range [13]. Mechanical properties especially the Charpy impact toughness at low temperature has been investigated and the use of DSS in cryogenic temperature has been assessed recently [14, 15]. Stress corrosion resistance at H<sub>2</sub>S is still a challenge in DSS [16]. Achieving good formability of DSS is also a challenge till now [17, 18]. Above all, finding more and more new application as well as replacing austenitic stainless steel need a better understanding of the properties of DSS.

The present paper reviews the design and manufacturing of duplex stainless steel focusing on the industrial application and suggests some of the future research areas in DSS.

## 2 Effect of Chemical Composition in DSS

Figure 1 shows the typical Scheffler diagram [19, 20] where ferrite and austenite stabilizers are plotted and the ratio of them decide the phase balance of particular chemistry during welding. This diagram is used for welding microstructure prediction and is not very accurate but useful for production and manufacturing technology. There are many other diagrams like Delong's constitutional diagram and WRC 1992 diagram [19, 20]. Later Scheffler diagram has been modified to predict the embrittlement phase during welding and thereby weldability of a composition.  $Cr_{eq}/Ni_{eq}$  has a significant impact on the microstructure of welded joint and simulated high

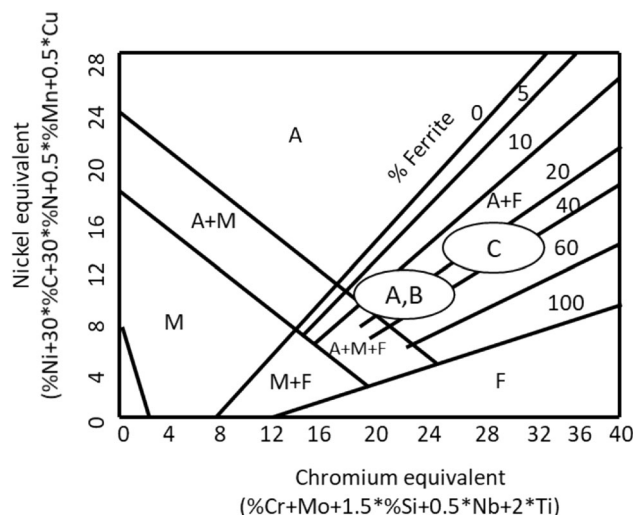


**Fig. 1** Scheffler's diagram showing the position of popular DSS (A, B: 2101, 2205, 2202 C: Super duplex)

temperature HAZ. Lowering of  $Cr_{eq}/Ni_{eq}$  can promote more austenite in the microstructure and also good pitting corrosion resistance and balanced mechanical properties. These diagrams do not include the effect of tungsten and nitrogen which is very important in terms of newly developed super duplex, hyper duplex DSS [21]. Brandi and Schön [22] recently calculated the effect of tungsten and nitrogen based on thermodynamic calculation and suggested that prefactor of 0.5 for tungsten and calculated nitrogen prefactor as high as 50 but due to inaccuracy of the calculation, they recommended the same prefactor to be 30. Also, they recommended that for intermetallic precipitation, the proper thermodynamic calculation needs to be done for better prediction of phase.

Thermocalc diagrams of popular duplex stainless steel have been shown in Fig. 2. Elemental partitioning of alloying elements occurs in different phases of DSS and that can effect the corrosion resistance of the alloys. Vannevik et al [23] suggested that Thermo-Calc is capable of predicting PRE-values as a function of temperature in ferrite and austenite. They correlated the Thermocalc

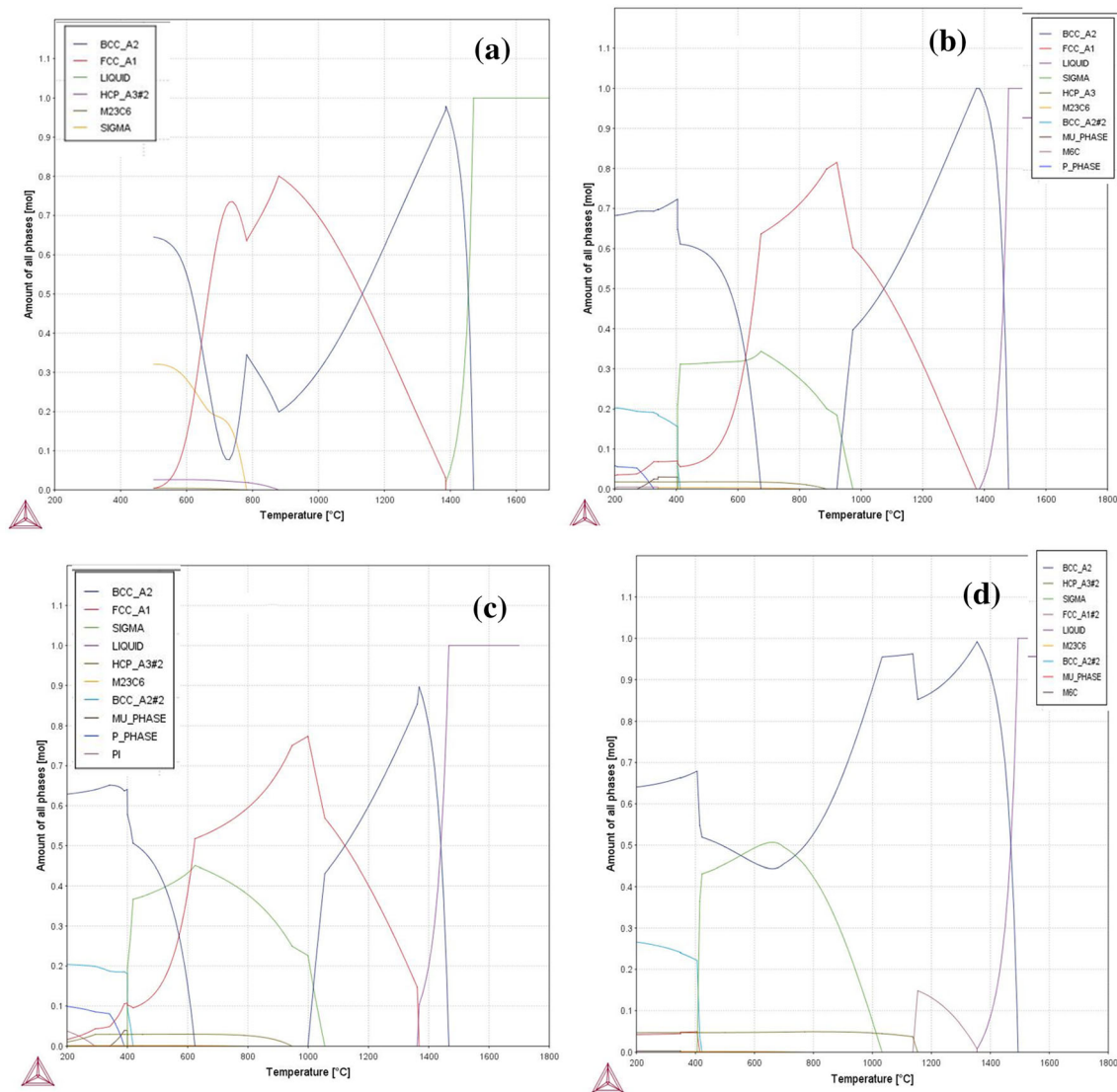


**Fig. 2** Thermocalc diagram showing phase fraction vs temperature in **a** 2101, **b** 2205, **c** 2507, **d** 2707 DSS

prediction and EPMA investigation and suggested preferential partitioning of chromium and molybdenum in ferrite and nitrogen to austenite. They further calculated the critical pitting temperature (CPT) and pitting resistance equivalent (PRE) from the formula and suggested that the weakest phase in terms of PRE can be the controlling phase for pitting.

The effect of different alloying elements popularly used in the DSS and their effect has been listed in Table 2. Generally, austenite stabiliser can not increase the strength and sometimes softens but can increase the Charpy impact toughness. Ferrite stabiliser increase the strength but deteriorate the impact toughness. Sulphur and boron can hamper the impact toughness [24].

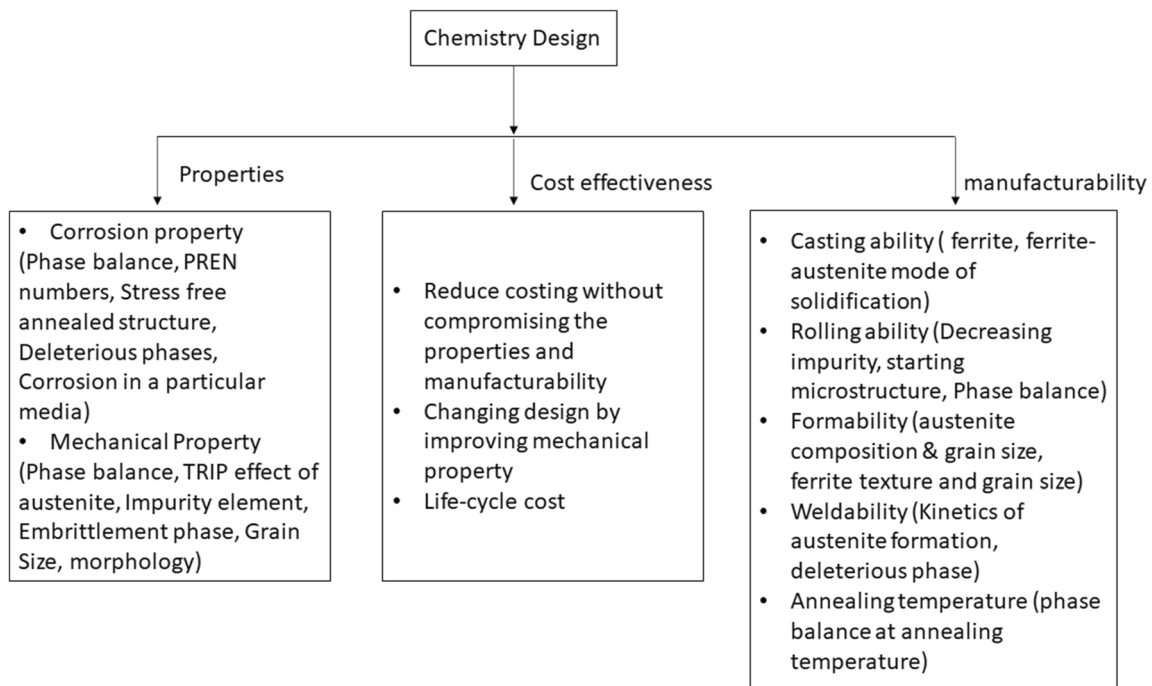
The chemistry design of duplex stainless steel is not only dependent on the mechanical property and corrosion

resistance of DSS but manufacturability also needs to be considered. Design factors considering the property, cost effectiveness and manufacturability have been schematically shown in Fig. 3. Sigma and Chi are the two embrittlement phases formed in duplex stainless steels. Sigma is an intermetallic phase of Fe, Cr and Mo and Chi phase is a precipitate phase with Fe, Cr and Mo in a varying stoichiometry. Time temperature and precipitation (TTP) diagram [20] for common duplex alloys has been shown in Fig. 4. As can be seen in the diagram that with increasing the chromium, molybdenum, and tungsten, sigma phase precipitation kinetics significantly increases.

With increasing the content of chromium, molybdenum and tungsten, the driving force for sigma formation increases, and also the curve shifts to a higher temperature which affects the processing of DSS. Lean duplex stainless

**Table 2** Role of popular alloying element in DSS [34, 35]

Alloying element	Solubility and stabilization	Role in corrosion	Role in mechanical property
Cr	BCC-100, FCC-12.5 and BCC stabilizer	General corrosion and pitting corrosion resistance and also increase nitrogen solubility	Little solid solution strengthening. Promotes $\sigma$ -phase precipitation strongly
Mn	BCC-3.5, FCC-100, FCC stabiliser	Decrease pitting corrosion resistance and increase nitrogen solubility	Little solid solution strengthening
Ni	BCC-6, FCC-100, FCC stabiliser	Little effect on general corrosion resistance	Solid solution softening, increase toughness, delay $\sigma$ -phase precipitation
Mo	BCC-31, FCC-1.7, BCC stabiliser	Increase pitting corrosion resistance and also increase little nitrogen solubility	Little solid solution strengthening. Promotes $\sigma$ -phase precipitation strongly
C	BCC:0.03, FCC:2.1, FCC stabiliser	Should be less for good corrosion resistance, Carbide formation can impact corrosion resistance	Increase solid solution strengthening
N	BCC:0.1, FCC:2.8, FCC stabiliser	Increase pitting corrosion resistance, Cr <sub>2</sub> N precipitation can hamper corrosion resistance	Increase solid solution strengthening without impacting ductility but if added higher amount austenite formation during solidification stage

**Fig. 3** Schematic diagram showing different factors of alloy design in DSS

steels are very safe in terms of sigma formation during processing and super and hyper duplex stainless steels are very much prone to sigma formation. The nucleation of sigma normally occurs at ferrite/ferrite boundary and ferrite/austenite interphase and they grow in the ferrite region [25–28]. As molybdenum fraction is higher in Sigma, diffusion of molybdenum will dictate the growth of sigma. Kinetics of the growth of the deleterious phases are very fast (5–10 min) in the nose temperature range and a

significant amount of sigma can form. The sequence of formation of deleterious phases in 2205 and 2507 is like Chromium nitrides,  $\chi$ -phase, and then  $\sigma$ -phase [29]. First, Chromium nitride forms and they provide the nucleation site for  $\chi$ -phase and eventually, both of them provide a nucleation site for  $\sigma$ -phase.

Sigma can consume the  $\chi$ -phase completely with higher time at the precipitation temperature range. While transforming the  $\sigma$ -phase, solute concentration in ferrite



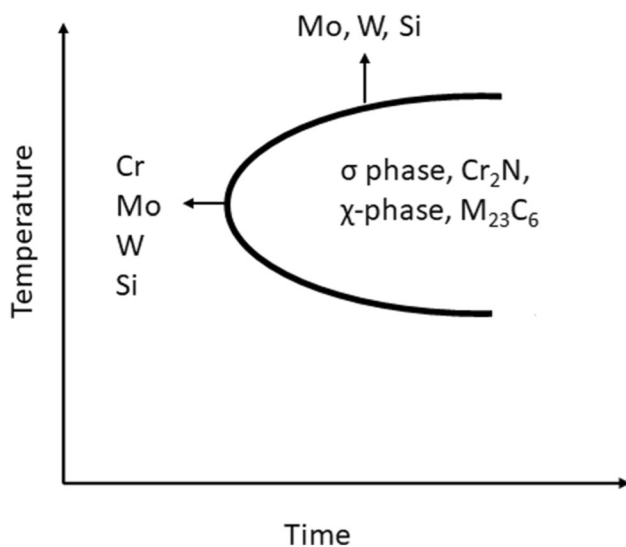


**Fig. 4** typical time–temperature precipitation (TPP) diagram in DSS [1, 4, 20]

depletes with Cr and Mo as they diffuse to richer  $\sigma$ -phase and thus ferrite becomes unstable and convert into secondary austenite [25, 27, 29, 30]. Back scattered Imaging in scanning electron microscopy is very effective for identifying the different phases due to the chemistry difference contrast in each phase [31]. Recently, Non-destructive techniques for detecting the sigma phase are going on, and by using Eddy current, ultrasonic sound, and electrochemical methods, sigma can be accurately detected [32]. This technology will be useful for metal production as well as fabricators.

In case of Hyperduplex stainless steel, the sigma formation nose is even higher due to the presence of higher Cr & Mo. The equilibrium phase is  $\sigma$ -phase and  $\text{Cr}_2\text{N}$ . Due to eutectoid reaction, the cellular structure of  $\sigma$ -phase and  $\text{Cr}_2\text{N}$  forms in hyper DSS at the initial stage of precipitation and with time they appear as blocky shape.  $\text{Cr}_2\text{N}$  is mostly round shaped but few rod shaped precipitate can be observed [7, 33]. Sometimes, segregation of Mo can take place due to improper casting at the centre region of slabs

and sigma can form preferentially at that segregated location as shown in Fig. 5.

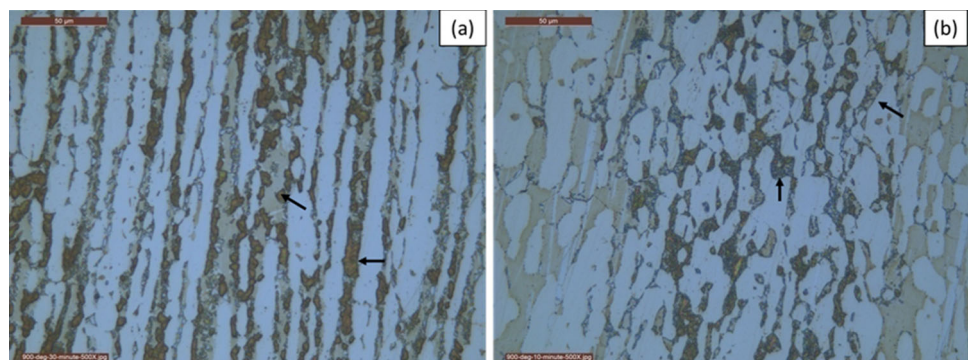
Sufficient amount of nitrogen is required to get higher austenite formation during welding cooling. The higher nitrogen content increases the kinetics of austenite formation and this also limits the  $\text{Cr}_2\text{N}$  precipitation as mostly nitrogen is consumed by the austenite precipitation. The resistance to pitting corrosion is usually considered to be controlled by the “weakest link”. In a low-nitrogen material, austenite will be attacked and with increased nitrogen content, nitrogen will strengthen the austenite and ferrite will be attacked. Nitrogen also hardens the austenite phase significantly thereby increasing the strength difference of ferrite and austenite significantly as per the hardness increment shown during deformation of 2101 DSS by Patra et al [10]. In comparison to austenitic stainless steel, nitrogen content in duplex stainless steel can’t influence the sigma phase precipitation. While in austenite, sigma formation get delayed by nitrogen addition due to lowering of the activity of Cr and Mo but nitrogen in DSS can not do that. Maybe more research in those areas is needed to identify the proper cause.

### 3 Microstructure and Mechanical Property Correlation

In general, the Flow stress of the duplex can be the weighted average of austenite and ferrite flow stress [36]. But, the yield strength of DSS is greater than both ferrite and austenite of the same composition. This can be due to the strengthening generated from the high lattice misorientation around the phase boundaries between austenite and ferrite (lattice parameter of austenite-0.257 nm and ferrite-0.248 nm) [37]. The high internal strain causes high mechanical strength. The tensile strength of DSS increases with increasing the austenite phase to 50 pct and decreases with further increment.

The ultrafine-grained 2205 duplex stainless steel has higher strength and plasticity than the coarse grained one.

**Fig. 5** Sigma phase precipitation under optical microscopy in **a** 2507 grade and **b** segregation of Mo induced sigma phase



The grain refinement of the 2205 duplex stainless steel inhibits the strain-induced  $\alpha'$ -martensite transformation and promotes to the formation of more nano twins [38].

Impact toughness of lamellar ferrite–austenite structure and inhomogeneously distributed austenite particle in ferrite matrix has been compared and it is found that lamellar microstructure can absorb more energy as crack deviates at the austenite–ferrite interface significantly due to delamination phenomenon [39]. Inhomogeneously distributed austenite particles can provide comparatively easy path for crack propagation [39]. (100) texture in ferrite also helps in the delamination process and improve the impact toughness [39].

Effect of embrittlement phase on the absorbed energy was also studied in details by Gennari et al [14] and as little as 2% of embrittlement phase can reduce the absorbed energy significantly. Coarse embrittlement phase can impact more severely than fine and dispersed particles. The particles are crack nucleating sites and can reduce the crack path and thereby reduce the impact toughness.

## 4 Corrosion Properties

Grain refinement can also improve the corrosion resistance of ultrafine 2205 duplex stainless steel in sodium chloride solution due to more protective passive layer formation in DSS [38]. Crevice corrosion resistance improves with the addition of tungsten in 25Cr containing DSS. The crevice attack initiates at  $\alpha/\gamma$  boundaries. In all cases,  $\alpha$  is selectively corroded; whereas dissolution of  $\gamma$  occurs at a later stage during crevice propagation [40]. The crevice corrosion resistance of 2304 DSS has been reported to decrease with increasing annealing temperature from 1030 to 1150 °C [41].

Nitrogen plays an important role in duplex stainless steel corrosion resistance. Nitrogen enhances the pitting potential at all PH solution but enhance the corrosion potential only in acid solution. The length scale and distribution of the austenite particles are not important for general and pitting corrosion resistance. In nitrogen containing DSS, the corroded structure is ferrite whereas without nitrogen steel, corroded structure is austenite. The mechanism of corrosion resistance is not clear for nitrogen but generally ammonium formation and nitrogen enrichment at the interface metal/passive film is considered for increasing pitting corrosion resistance [42].

The pitting corrosion resistance with varying %ferrite content is closely related to the galvanic corrosion rate between ferrite and austenite phase and thus almost highest pitting potential is observed at about 55%ferrite volume fraction. Stable corrosion resistance can be determined by the pit growth rate rather than pit initiation probability [42].

Ferritic and austenitic microstructure together in DSS can be beneficial for Chloride stress corrosion resistance compared to popular 304L and 316L grade. Electrochemical and mechanical synergy between ferrite and austenite may be the reason for good corrosion resistance to chloride SCC [43]. Liu et al [44] investigated the SCC of 2205 DSS in CO<sub>2</sub>-H<sub>2</sub>S environment and concluded that SCC susceptibility of 2205 increases in saturated test solution of CO<sub>2</sub> and H<sub>2</sub>S. Entrapment of Hydrogen can deteriorate the corrosion resistance as DSS is prone to hydrogen induced cracking.

## 5 Manufacturing

### 5.1 Casting

Most of the DSS solidify in the ferritic mode and during cooling transform into ferrite and austenite. Ferritic solidification is not difficult as impurities is soluble in ferrite. In the as cast structure, mainly coherent or semi-coherent interphase boundaries can be observed where ferrite and austenite follow Kurdjumov–Sachs (K–S) or Nishiyama–Wassermann (N–W) orientation relationship (OR) [10, 12, 45]. EBSD inverse pole figure map of as-cast and hot-rolled samples is presented in Fig. 6. In cast sample, K–S orientation relationship is observed between  $\gamma$  and  $\delta$ , across the interphase boundaries (Fig. 6b). As the samples are hot deformed by 30%, the nature of the austenitic phase become spherical (Fig. 6c) and the interphase boundaries surrounding large and deformed  $\gamma$ -regions become incoherent and deviate from ideal K–S OR as shown by ‘green’ lines in Fig. 6d. As the deformation progresses, the slip transfer between ferrite to austenite increases and interphases become incoherent.

### 5.2 Hot Deformation

Normally hot ductility of DSS is poor and edge crack appears during hot rolling. Hot ductility of popular 2205 grade is higher than both 2101 lean duplex and super duplex stainless steel. Hot ductility of Lean duplex is poorest among the popular duplex stainless steels. This may be due to the strength difference of ferrite and austenite is higher in 2101 owing to comparatively higher

nitrogen content. Super duplex stainless steel also suffer from low hot ductility and also the hot processing window is short due to the embrittlement phase starts below 950 °C. Generally, the poor hot ductility of DSS is correlated to the different hot strength of ferrite and austenite and nature of interphase boundaries [12]. Strain partitioning has also been reported with strain accumulation in comparatively

softer ferrite phase and stress concentration at interphase boundaries as austenite is harder. Interphase sliding is the only method by which the stress concentration can be released but in the as cast condition, interphase boundary sliding become difficult due to coherent nature and they try to maintain the special atomic arrangement (Fig. 6).

To avoid hot-cracking in DSS, high deformation temperature and low strain rate was suggested for hot rolling [10–12, 46–50]. However, high-temperature industrial processing requires high-temperature soaking of as-cast slab, which is very difficult in DSS as ferrite phase predominantly appears at higher temperature and soaking at high temperature leads to slab bending. The facility for soaking at very high temperature is also not available in several rolling mills. Use of very low strain-rate also hampers the productivity as well as temperature. Dynamic recrystallization of austenite (above 900 °C) and Continuous dynamic recrystallization of Ferrite (above 900 °C) takes place during hot deformation. Below 900 °C, no softening is observed and material accumulates lot of strain inside the matrix [10]. With increasing the strain, significant discontinuous dynamic recrystallization takes place with the formation of annealing twins. Predominantly cube texture appears inside the ferrite phase which may have originated during the casting stage. As the ferrite deforms through Continuous dynamic recrystallization, the texture does not significantly change with processing. Whereas austenite transforms to mostly deformation texture while hot deformation [10].

Strain-induced precipitation of secondary austenite can form during hot deformation in 2101 DSS as they contain higher nitrogen content. Higher nitrogen content can increase the kinetics of austenite formation and thus small island of strain free secondary austenite forms inside the ferrite matrix. The precipitation process increases with the decrease in deformation temperature and with the increase in applied strain. The transformed austenite maintains mostly K–S orientation relationship with the ferrite matrix. Figure 7a shows the K–S interphase map of a hot deformed sample at 900 °C with 0.8 strain and small austenite particles are shown by red arrows and Fig. 7b shows the crack propagation through the small austenite particles. Thus, sliding of K–S interphase boundaries are difficult during hot deformation and crack propagates through them.

In a recent paper excellent better hot formability has been achieved by supercooled  $\delta$  ferrite phase formation before hot working by using rapid cooling from the initial reheating temperature to the hot working temperature. As the ferrite phase is softer than austenite, retaining of ferrite phase at the deformation temperature can improve the hot ductility. This thermomechanical processing technology can be implemented by installing cooling equipment immediately before hot working [51]. But may be difficult to apply industrially, specially for high nitrogen-containing grades, diffusion of nitrogen is faster and austenite formation will take place very quickly during hot rolling and they will maintain the K–S Orientation relationship and thereby decrease the ductility [12].

**Fig. 6** EBSD phase map of as-cast condition (a) and 30% rolled condition (c). EBSD orientation maps of interphase boundaries with respect to angular deviation ( $< 10^\circ$  represented in ‘red’ colour and  $> 10^\circ$  represented in ‘green’ colour) from ideal Kurdjumov–Sachs (K–S) orientation relationship across the boundary for as cast (b) and 30% deformed (d) (colour figure online)

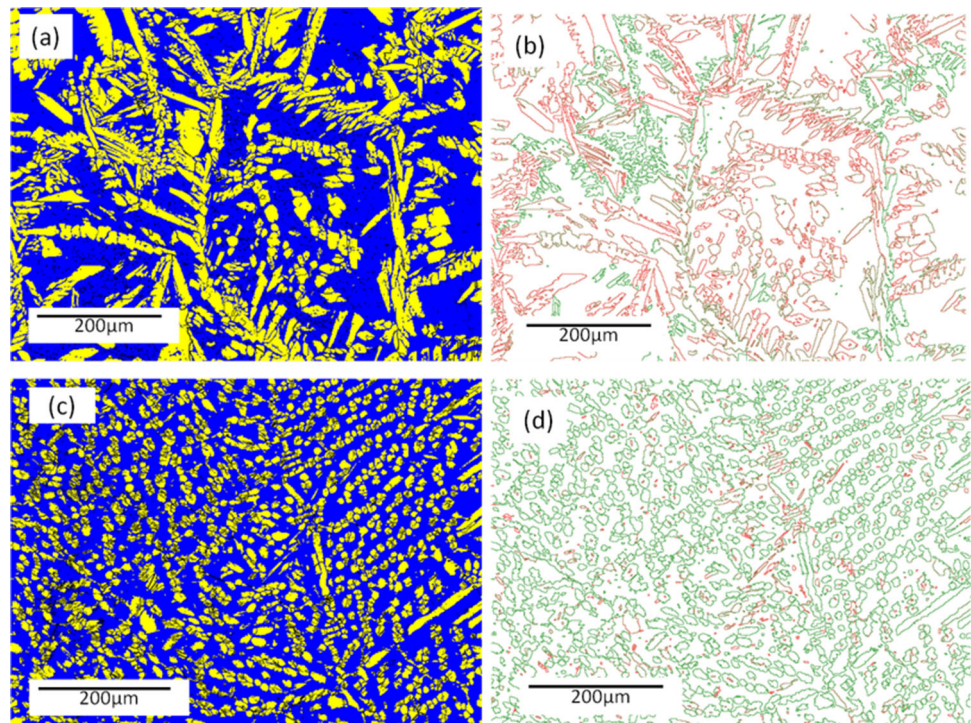
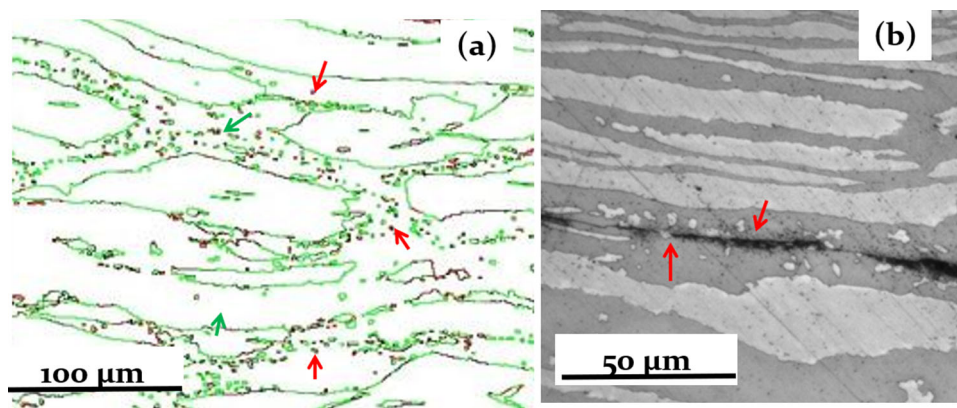




**Fig. 7** Cracking at K–S interphase boundaries between ferrite and austenite **a** deformed at 900 °C (black colour boundaries represent  $< 2^\circ$  deviation from K–S, red colour:  $2^\circ$ – $7^\circ$ , Green colour:  $> 7^\circ$ ), **b** industrially edge crack sample [12]



Recent study was carried out using the rare earth element for increasing the hot ductility and they concluded that rare earth narrows down the hot working parametric regions for the presence of this particular phenomenon. RE reduces the mismatch in hardness between ferrite and austenite. This result suggests that RE can improve the hot workability of DSSs to a certain extent. RE can help to increase the level of DRX [52].

### 5.3 Forming

Cold forming of DSS has been studied by several researchers and two major problems have been identified: firstly high spring back due to high yield strength and lower formability due to lower elongation. Outokumpu recently developed a higher formable DSS by adjusting the chemical composition where austenite of the DSS can transform to martensite during forming and thereby providing good elongation. The TRIP-effect offers a balanced work hardening rate resulting in an enhanced uniform elongation and higher work hardening ratio at large (plastic) deformations in comparison to other duplex grades. These mechanical properties make the TRIP DSS grades more suitable for the manufacturing of components with stretch forming as the primary forming operation [18].

During the deep drawing process, the hardness difference of the two phases can create the problem. Being harder, the austenite phase can exert pressure on the phase boundary and restrict its elongation. Also, phase boundary has large misorientation which restricts the dislocation motion and also coordinated deformation of two phases. As the strain is in-homogeneously distributed, cracking or wrinkling can appear. And deep drawability is poor in 2507 grade [17].

## 6 Application

The use of DSS in the chemical industry has been increased as DSS not only possesses good corrosion resistance but also better SCC and mechanical property than austenitic stainless steel. Duplex can be used in Chloride SCC, ammonium carbamate solution, strongly alkaline chloride bearing solution and oxygen-free carbamate solution. DSS also can replace the urea grades. Use of DSS is very beneficial in those environments [16]. Duplex stainless steel has been extensively used as electrode in copper refining as it replaces 316L grade due to better corrosion resistance and mechanical properties.

### 6.1 Chemical Storage Tank

S32101 was chosen as the material for construction of this storage tank over 316L stainless steel due to increased strength and resistance to chloride SCC. Because of the high strength of the lean duplex, the wall thickness was reduced for three of the six elevations over 316L, reducing material weight and resulting in a 10% material reduction for the tank walls [16]. The life cycle cost of a storage tank

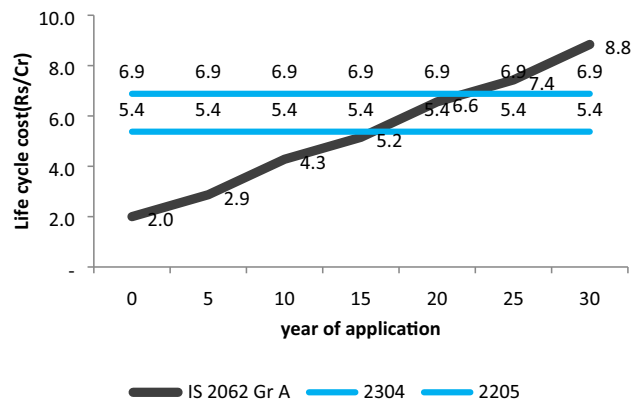


**Fig. 8** life cycle cost evaluation for different grades in a storage tank application



in the coastal atmosphere has been shown in Fig. 8 by replacing IS2062 grade with 2304/2205 DSS.

## 6.2 Heat Exchanger

Heat exchangers are the critical components for many industries, particularly in chemical and oil and gas plants. Due to their extremely high corrosion resistance and cost-effectiveness, super duplex stainless steels can replace Titanium for seawater cooled heat exchangers. High corrosion resistance of the super duplex alloys in a wide range of fluid makes it suitable for using in wide range of cooling duties [53].

## 6.3 Pulp & Paper Plant

All varieties of duplex including lean duplex S32101, duplex 2205, and super duplex S32760 and S32750 have been used at a pulp and paper plant. Lean duplex S32101 can be used for various capacities including a black liquor tank and a caustic tank. Lean duplex replaces 300 series stainless steels in evaporators due to its high strength and good resistance to chloride SCC. Standard duplex 2205 is used in various process vessels. Super duplex S32760 and S32750 are used in various acid tanks including sulfuric acid and sodium chlorite [1, 16].

## 6.4 Batch Digesters & Continuous Digester

Due to higher strength and corrosion resistance, 2205 & 2304 have been used instead of 304L and 316L grade in batch and continuous digester and can reduce wall thickness [53].

## 6.5 Nuclear Power Plant

Recently, super duplex stainless steel has been used in nuclear power plant construction. The reactor coolant pump has been manufactured using super duplex stainless steels due to their resistance to the corrosive tropical sea environment.

## 7 Conclusion

Duplex Stainless steel has been chosen as an effective alternative to popular austenitic stainless steels in many critical applications due to its superior mechanical property and corrosion resistance. Chemical composition design should consider the important contribution of embrittlement phase formation and manufacturability. Deep drawing or forming is not easy in DSS and needs further improvement. Mechanical properties can be improved by

applying thermomechanical processing but poor hot ductility is a challenge specially in case of high nitrogen-containing grades. K–S orientation relationship in the as-cast structure as well as between the stain-induced austenite and ferrite boundaries hampers the hot ductility of the DSS. Further studies on formability and corrosion are needed for expanding the application of DSS.

**Acknowledgements** Authors are grateful to Dr. L. K. Singhal for his valuable suggestions during preparation of the manuscript.

## References

- [1] J. Charles: *Steel Res. Int.*, 2008, vol. 79, pp. 455–65.
- [2] J. Charles: 2015, pp. 1–5.
- [3] No Title, <https://www.marketsandmarkets.com/Market-Reports/duplex-stainless-steel-market-32316483.html>.
- [4] J. Charles and S. Bernhardtsson: in *Duplex Stainless Steels Conference (DSS); 1991; Beaune*, J. Charles, ed., Éd. de Physique, Beaune, Bourgogne, France, 1991, pp. 151–68.
- [5] Outokumpu: *Sandvikens Tryckeri*, 2013, pp. 1–89.
- [6] J.-O. Nilsson: *Mater. Sci. Technol.*, 1992, vol. 8, pp. 685–700.
- [7] G. Chail and P. Kangas: *Procedia Struct. Integr.*, 2016, vol. 2, pp. 1755–62.
- [8] G. Notten: *Duplex Stainless Steel 97-5th world conference series*, pp. 9–16.
- [9] A. Belyakov, R. Kaibyshev, and R. Zaripova: *Mater. Sci. Forum*, 1993, vol. 113–115, pp. 385–90.
- [10] S. Patra, A. Ghosh, L.K. Singhal, A.S. Podder, J. Sood, V. Kumar, and D. Chakrabarti: *Metall. Mater. Trans. A Phys. Metall. Mater. Sci.*, DOI:<https://doi.org/10.1007/s11661-016-3759-1>.
- [11] M. Ve, G. Martin, S. Kumar, Y. Bre, L. Delannay, T. Pardoën, and J. Mithieux: 2012, vol. 60, pp. 4646–60.
- [12] S. Patra, A. Ghosh, V. Kumar, D. Chakrabarti, and L.K. Singhal: *Mater. Sci. Eng. A*, 2016, vol. 660, pp. 61–70.
- [13] S. Hertzman and J. Charles: *Rev. Metall. Cah. D'Informations Tech.*, 2011, vol. 108, pp. 413–25.
- [14] C. Gennari, L. Pezzato, E. Piva, R. Gobbo, and I. Calliari: *Mater. Sci. Eng. A*, 2018, vol. 729, pp. 149–56.
- [15] K. Yildizli: *Mater. Des.*, 2015, vol. 77, pp. 83–94.
- [16] N. Dsm and E. Stamicarbon: 1997, pp. 9–16.
- [17] Z. Gao, J. Li, and Y. Wang: *ISIJ Int.*, 2019, vol. 59, pp. 531–40.
- [18] A. Groth, E. Schedin, C.C. Sun, H. He, and L. Guan: *J. Phys. Conf. Ser.*, DOI:<https://doi.org/10.1088/1742-6596/896/1/012013>.
- [19] D.J. Kotecki and T. a. Siewert: *AWS Annu. Meet.*, 1992, pp. 171–8.
- [20] S. Hertzman and J. Charles: *Rev. Métallurgie*, 2011, vol. 108, pp. 413–25.
- [21] Y. Jiang, H. Tan, Z. Wang, J. Hong, L. Jiang, and J. Li: *Corros. Sci.*, 2013, vol. 70, pp. 252–9.
- [22] S.D. Brandi and C.G. Schön: *J. Phase Equilibria Diffus.*, 2017, vol. 38, pp. 268–75.
- [23] H. Vannevik, J.O. Nilsson, J. Frodigh, and P. Kangas: *ISIJ Int.*, 1996, vol. 36, pp. 807–12.
- [24] H.Y. Liou, Y.T. Pan, R.I. Hsieh, and W.T. Tsai: *J. Mater. Eng. Perform.*, 2001, vol. 10, pp. 231–41.
- [25] H. Sieurin and R. Sandström: *Mater. Sci. Eng. A*, 2007, vol. 444, pp. 271–6.
- [26] C.-C. Hsieh and W. Wu: *ISRN Metall.*, 2012, vol. 2012, pp. 1–16.

- [27] Vahid Hosseini: *Super Duplex Stainless Steels: Microstructure and Properties of Physically Simulated Base and Weld Metal*, 2018.
- [28] K. Nishimoto, K. Saida, and O. Katsuyama: *Weld. World*, 2006, vol. 50, pp. 13–28.
- [29] H. Zhao, Z. Zhang, H. Zhang, J. Hu, and J. Li: *J. Alloys Compd.*, 2016, vol. 672, pp. 147–54.
- [30] H. Keshmiri and M. Shahhosseini: 2008.
- [31] N. Llorca-Isern, H. López-Luque, I. López-Jiménez, and M.V. Biezma: *Mater. Charact.*, 2016, vol. 112, pp. 20–9.
- [32] M. V. Biezma, U. Martin, P. Linhardt, J. Röss, C. Rodríguez, and D.M. Bastidas: *Eng. Fail. Anal.*, 2021, vol. 122, p. 105227.
- [33] L. Karlsson: *Weld. World*, 2012, vol. 56, pp. 65–76.
- [34] X. Li: UNSW Sidney, 2019.
- [35] M. Knyazeva and M. Pohl: *Metallogr. Microstruct. Anal.*, 2013, vol. 2, pp. 113–21.
- [36] M. Pan, X. Zhang, P. Chen, X. Bin Su, and R.D.K. Misra: *Mater. Sci. Eng. A*, 2020, vol. 788, p. 139540.
- [37] M. Okayasu and D. Ishida: *Metall. Mater. Trans. A Phys. Metall. Mater. Sci.*, 2019, vol. 50, pp. 1380–8.
- [38] L. Jinlong, L. Tongxiang, W. Chen, and D. Limin: *Mater. Sci. Eng. C*, 2016, vol. 62, pp. 558–63.
- [39] N. Haghdad, P. Cizek, P.D. Hodgson, and H. Beladi: *Mater. Sci. Eng. A*, 2019, vol. 745, pp. 369–78.
- [40] C. Torres, R. Johnsen, and M. Iannuzzi: *Corros. Sci.*, 2021, vol. 178, p. 109053.
- [41] D. Han, Y. Jiang, C. Shi, Z. Li, and J. Li: *Corros. Sci.*, 2011, vol. 53, pp. 3796–804.
- [42] G. Lothongkum, P. Wongpanya, S. Morito, T. Furuhashi, and T. Maki: *Corros. Sci.*, 2006, vol. 48, pp. 137–53.
- [43] P. Kangas and J.M. Nicholls: *Mater. Corros.*, 1995, vol. 46, pp. 354–65.
- [44] Z.Y. Liu, C.F. Dong, X.G. Li, Q. Zhi, and Y.F. Cheng: *J. Mater. Sci.*, 2009, vol. 44, pp. 4228–34.
- [45] C. Herrera, D. Ponge, and D. Raabe: *steel Res. Int.*, 2008, vol. 79, pp. 482–8.
- [46] J. Liu, G.W. Fan, P. De Han, J.S. Liu, J.Q. Gao, and J.F. Yang: *Mater. Sci. Forum*, 2009, vol. 620–622, pp. 161–4.
- [47] E. Evangelista, H.J. McQueen, M. Niewczas, and M. Cabibbo: 2004, vol. 43, pp. 339–53.
- [48] M. Bartei, E. Evangelista, H.J. McQueen, and B. Verlinden: *La Metall. Ital.*, 2000, vol. 9, pp. 37–44.
- [49] J. Cabrera, A. Mateo, L. Llanes, J.M. Prado, and M. Anglada: *J. Mater. Process. Technol.*, 2003, vol. 143–144, pp. 321–5.
- [50] Y.L. Fang, Z.Y. Liu, W.Y. Xue, H.M. Song, and L.Z. Jiang: 2010, vol. 50, pp. 286–93.
- [51] S. Sasaki, T. Katsumura, and J. Yanagimoto: *J. Mater. Process. Technol.*, 2020, vol. 281, p. 116614.
- [52] T. Zhou, Y. Xiong, X. Zha, Y. Yue, Y. Lu, T. He, F. Ren, E. Rani, H. Singh, J. Kömi, M. Huttula, and W. Cao: *J. Mater. Res. Technol.*, 2020, vol. 9, pp. 8379–90.
- [53] Z. Schulz, P. Whitcraft, and D. Wachowiak: *NACE - Int. Corros. Conf. Ser.*, 2014, pp. 1–10.

**Publisher's Note** Springer Nature remains neutral with regard to jurisdictional claims in published maps and institutional affiliations.